Chinese Journal of Oceanology and Limnology
Vol. 33 No. 3, P. 741-747, 2015
http://dx.doi.org/10.1007/s00343-015-3357-x

Particulate organic carbon export fluxes on Chukchi Shelf, western Arctic Ocean, derived from $^{210}Po/^{210}Pb$ disequilibrium*

HE Jianhua (何建华)[1, 2, 3], YU Wen (余雯)[2], LIN Wuhui (林武辉)[2, 3, 4], MEN Wu (门武)[2], CHEN Liqi (陈立奇)[2, 3, **]

[1] *College of Oceanography and Environment Science, Xiamen University, Xiamen 361005, China*

[2] *Third Institute of Oceanography, State Oceanic Administration, Xiamen 361005, China*

[3] *Key Lab of Global Change and Marine-Atmospheric Chemistry, State Oceanic Administration, Xiamen 361005, China*

[4] *Department of Engineering Physics, Tsinghua University, Beijing 100084, China*

Received Jan. 19, 2014; accepted in principle Apr. 8, 2014; accepted for publication Aug. 27, 2014

Abstract Fluxes of particulate organic carbon (POC) were derived from $^{210}Po/^{210}Pb$ disequilibrium during the 4th Chinese National Arctic Research Expedition (CHINARE-4) from July 1 to September 28, 2010. Average residence times of particulate ^{210}Po in the euphotic zone were -16.00 a to 1.54 a, which are higher than those of dissolved ^{210}Po (-6.89 a to -0.70 a). Great excesses of dissolved ^{210}Po were observed at all stations, with an average $^{210}Po/^{210}Pb$ ratio of 1.91±0.20, resulting from ^{210}Pb atmospheric deposition after sea ice melt. POC fluxes from the euphotic zone were estimated by two methods (E and B) in the irreversible scavenging model. Estimated POC fluxes were 945–126 mmol C/(m^2·a) and 1 848–109 mmol C/(m^2·a) by methods E and B, respectively, both decreasing from low to high latitude. The results are comparable to previous works for the same region, indicating efficient biological pumping in the Chukchi Sea. The results can improve understanding of the carbon cycle in the western Arctic Ocean.

Keyword: particulate organic carbon (POC) flux; $^{210}Po/^{210}Pb$ disequilibrium; Chukchi Shelf

1 INTRODUCTION

About 30% of anthropogenic CO_2 is taken up by the ocean, especially the Arctic and Southern oceans, owing to high biological production in the large ocean margin areas and low temperatures (Cai et al., 2010). The Chukchi Shelf is one of the most productive continental shelves in the Arctic Ocean and is important in carbon sequestration (Woodgate et al., 2005; Yu, 2010). The magnitude of atmospheric CO_2 absorbed in these areas has been of concern to oceanographers worldwide (Baskaran et al., 1995; Anderson et al., 1998; Pipco et al., 2002; Bates et al., 2006; Liu et al., 2007; Else et al., 2008).

As an interface for exchange of CO_2 between the surface ocean and interior ocean, the euphotic zone plays a key role in the growth, removal and cycling of biomass. Fluxes within the euphotic zone of carbon, nutrients and other associated elements involved in biogeochemical cycles are very important in the study of global CO_2 (Yang et al., 2004; He et al., 2008). Radioactive isotopes, especially natural particle-reactive radionuclides (e.g., ^{234}Th and ^{210}Po) provide another possible means for quantifying export flux of particulate organic carbon (POC) from the surface ocean at various time scales, because of their specific half-lives (Verdeny et al., 2009; Stewart et al., 2011).

Both ^{210}Po and ^{210}Pb are progeny of the ^{238}U decay chain, and are naturally occurring particle-reactive radionuclides. ^{210}Pb ($t_{1/2}$=22.3 a) is produced in situ by decay of its longer-lived grandparent ^{226}Ra and from atmospheric deposition, whereas ^{210}Po is supplied

* Supported by the National Natural Science Foundation of China (Nos. 41106167, 11205094, 41230529, 41476172, 41406221, 41476173), the Youth Foundation of State Oceanic Administration (No. 2011531), and the CHINARE2012-15 for 01-04-02, 02-01, and 03-04-02
** Corresponding author: lqchen@soa.gov.cn

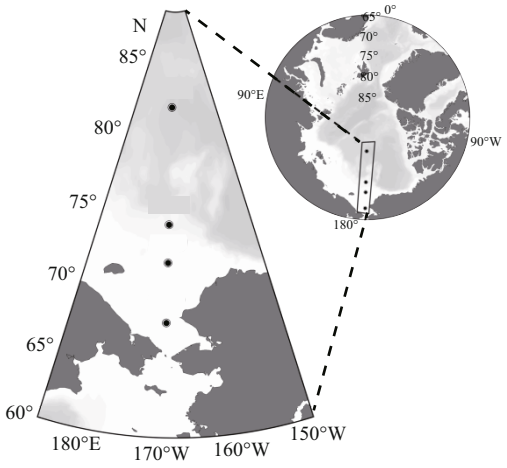

Fig.1 Study area and sampling stations

almost exclusively in situ by the decay of its grandparent ^{210}Pb, with a minor additional source from atmospheric deposition (Baskaran, 2011). Although ^{210}Pb and ^{210}Po are particle-reactive radionuclides, the preferential uptake of ^{210}Po by plankton and its transfer in the food chain can be used to quantify organic carbon fluxes (Carvalho, 2011; Kim et al., 2012). Furthermore, export on a timescale of several months can be derived by ^{210}Po/^{210}Pb disequilibrium, longer than the several weeks of ^{234}Th/^{238}U disequilibrium (Friedrich et al., 2002).

In this study, we estimated ^{210}Po-derived export fluxes of POC from the euphotic zone at different stations during the 4th Chinese National Arctic Research Expedition (CHINARE-4).

2 MATERIAL AND METHOD

2.1 Location and sample collection

During CHINARE-4 from July 1 to September 20, 2010, a conductivity, temperature and depth (CTD) rosette (SEABIRD 911/17) was used to collect 10-L seawater samples at various depths in the upper 0–100 m water column at four stations in the Arctic Ocean, for analysis of ^{210}Po and ^{210}Pb. At stations R03 and R09, sampling was done during July 21–24, whereas that at R12 and R20 was during August 24–29. A map of the study area and stations is provided in Fig.1.

One liter of each 10-L seawater sample was filtered through a pre-combusted (450°C, 2 h) 0.45-μm QMA membrane immediately after sampling, and then particles and the filter were sealed inside tin foil and stored frozen for subsequent POC analysis. The remaining nine liters of seawater from each sample were filtered through a 0.45-μm membrane filter (120 mm diameter), to obtain dissolved samples and particulate samples. After filtration, dissolved samples were acidified to pH 1 with concentrated HCl. All samples were stored until laboratory analysis of POC, ^{210}Po and ^{210}Pb.

2.2 Radionuclide analysis

For dissolved and particulate ^{210}Po and ^{210}Pb, the analytical methods used followed the modifications of Nozaki (1986) and Masque et al. (2002). Briefly, filter samples were digested using sequential aqua regia, HNO_3 and HCl, with $HClO_4$ and HF, and the dissolved material was eventually taken up in 1.5 mol/L HCl. During digestion, samples were spiked with ^{209}Po as a yield tracer and stable lead as a recovery tracer. The dissolved ^{210}Po was co-precipitated with $Fe(OH)_3$ and redissolved with 1 mol/L HCl. Po was plated onto nickel discs using stirring hot plates and counted on a low background alpha spectrometer (Canberra 7200-08; CT,USA). The plating solution was then replated to remove any residual ^{210}Po and ^{209}Po, then re-spiked with ^{209}Po and retained for at least 6 months for ingrowth of ^{210}Po to determine ^{210}Pb. Pb yields were determined through measurement of stable Pb by inductively coupled plasma mass spectrometry (ICP-MS), and recovery was generally between 80% and 90%. The ^{210}Po and ^{210}Pb activities were decay-corrected to the time of sampling according to Fleer and Bacon (1984).

3 RESULT AND DISCUSSION

3.1 Distribution of particulate and dissolved ^{210}Po and ^{210}Pb

The activity of ^{210}Po and ^{210}Pb in different phases and the activity ratio ^{210}Po/^{210}Pb)$_{A.R}$ are given in Table 1. Vertical profiles of ^{210}Po/^{210}Pb)$_{A.R}$ in different water columns are shown in Fig.2. The average dissolved ^{210}Pb of various stations shows an increasing trend from 1.12 to 1.78 Bq/m^3 northward from July to August, which may have resulted from atmospheric deposition of ^{210}Pb during ice melt. The average particulate ^{210}Pb (2.22 Bq/m^3) was higher than the dissolved ^{210}Pb (1.49 Bq/m^3), indicating intense particle scavenging of ^{210}Pb (Bacon et al., 1976; Shimmield et al., 1995).

The vertical profile of POC in different water columns and relationship between POC content and particulate Po are shown in Fig.3. The average content of POC decreased northward. However, the highest

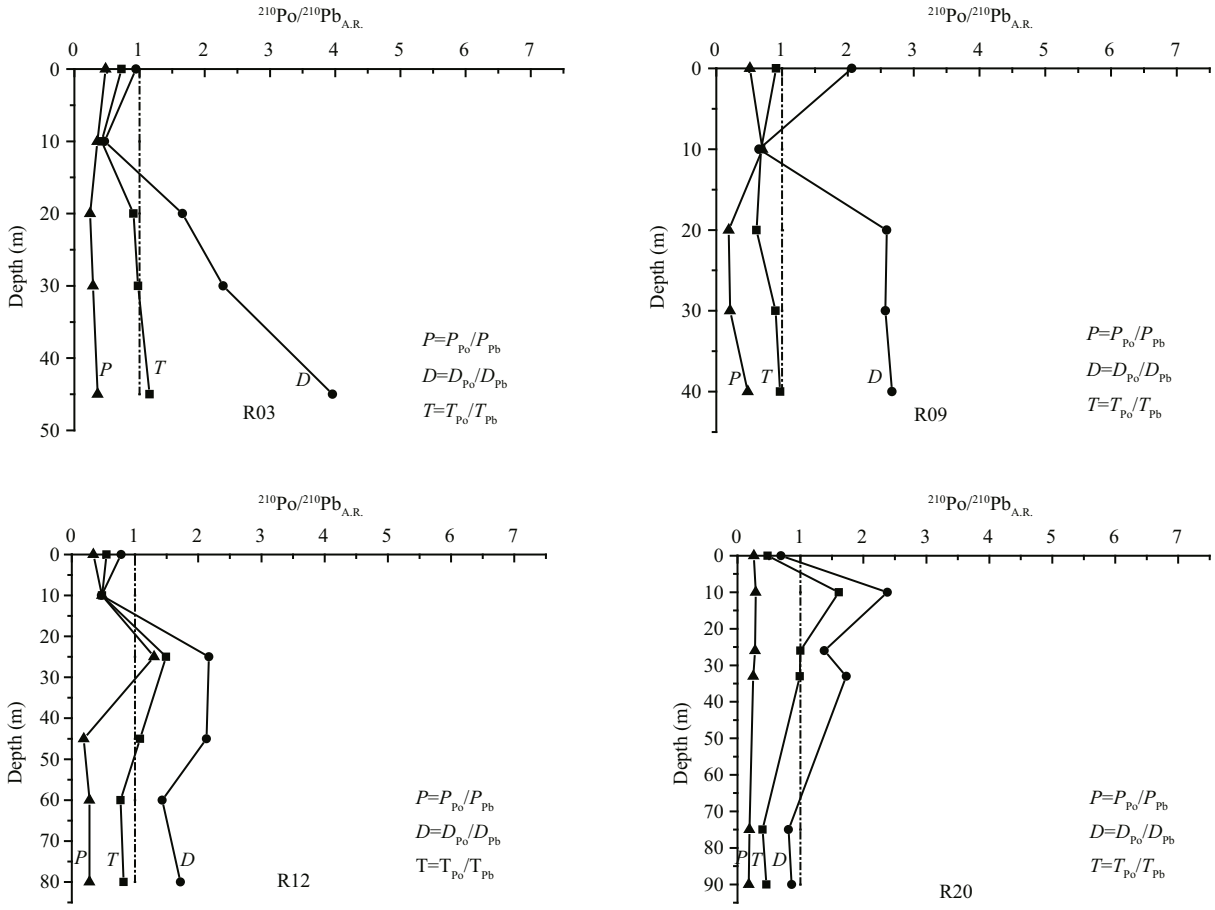

Fig.2 Vertical profiles of ^{210}Po, ^{210}Pb and POC in different water columns

P, *D*, and *T* represent particulate, dissolved, and total ^{210}Po or ^{210}Pb, respectively. $^{210}Po/^{210}Pb_{AR}$ is activity ratio of ^{210}Po to ^{210}Pb

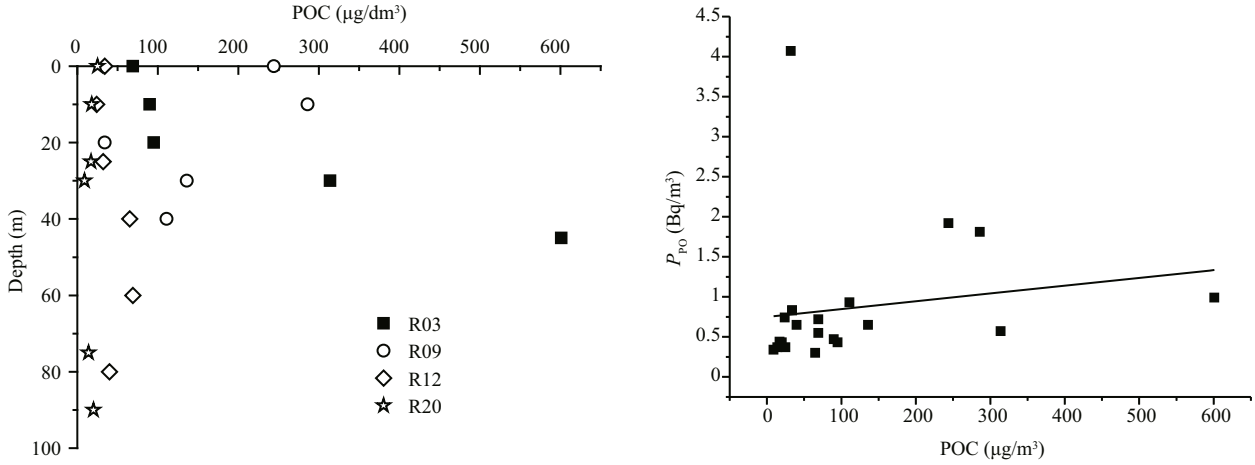

Fig.3 Vertical profile of POC in different water columns and relationship between POC content and particulate Po

value for surface water appeared at R09, perhaps caused by ice melt, which resulted in biomass bloom from the bottom ice (Yu et al., 2012). Positive correlation (R^2=0.027) between POC content and particulate Po confirms that Po may be used as a tracer of POC export.

3.2 Total Po and Pb, residence time of ^{210}Po, water-column disequilibrium and flux

The half-life of ^{210}Po constrains the seasonal time scale of disequilibrium of $^{210}Po/^{210}Pb$ for quantifying the export fluxes of POC. Boundary scavenging,

Table 1 POC content, ^{210}Po and ^{210}Pb activity, and Po/Pb ratio in water column samples

Station No.	Latitude	Longitude	Depth (m)	POC	D_{Po}	P_{Po}	T_{Po}	D_{Pb}	P_{Pb}	T_{Pb}	$^{210}Po/^{210}Pb_{A.R.}$		
				(μg/dm^3)	(Bq/m^3)						D	P	T
R03	68°N	169°W	0	69	1.19±0.20	0.55±0.05	1.73±0.14	1.26±0.13	1.14±0.16	2.40±0.23	0.94±0.10	0.48±0.05	0.72±0.07
			10	90	0.88±0.12	0.47±0.05	1.35±0.15	1.91±0.19	1.33±0.14	3.24±0.30	0.46±0.05	0.35±0.04	0.42±0.04
			20	95	2.64±0.30	0.43±0.05	3.08±0.35	1.59±0.17	1.80±0.16	3.40±0.33	1.66±0.12	0.24±0.02	0.91±0.10
			30	314	2.45±0.25	0.57±0.06	3.02±0.33	1.07±0.09	2.02±0.19	3.09±0.30	2.28±0.23	0.28±0.03	0.98±0.10
			45	601	3.13±0.35	0.99±0.10	4.12±0.40	0.79±0.80	2.78±0.26	3.57±0.37	3.96±0.40	0.36±0.03	1.15±0.12
R09	72°N	169°W	0	244	2.68±0.22	1.92±0.21	4.59±0.50	1.30±0.12	3.73±0.38	5.03±0.52	2.06±0.20	0.51±0.05	0.91±0.10
			10	286	0.97±0.79	1.81±0.17	2.78±0.31	1.49±0.16	2.57±0.25	4.06±0.40	0.65±0.06	0.70±0.07	0.68±0.07
			20	34	2.47±0.28	0.83±0.10	3.30±0.31	0.95±0.11	4.46±0.46	5.41±0.53	2.59±0.26	0.19±0.02	0.61±0.06
			30	136	3.36±0.28	0.65±0.10	4.00±0.38	1.31±0.11	3.13±0.31	4.44±0.46	2.57±0.26	0.21±0.02	0.90±0.09
			40	111	1.53±0.10	0.93±0.11	2.46±0.25	0.57±0.06	1.95±0.20	2.52±0.20	2.67±0.26	0.48±0.04	0.97±0.10
R12	74°N	169°W	0	34	1.72±0.16	0.83±0.08	2.55±0.26	2.19±0.25	2.44±0.26	4.63±0.43	0.78±0.08	0.34±0.03	0.55±0.05
			10	24	1.33±0.10	0.74±0.08	2.07±0.26	2.79±0.30	1.55±0.13	4.34±0.43	0.47±0.46	0.48±0.05	0.48±0.05
			25	32	1.94±0.26	4.07±0.45	6.01±0.68	0.89±0.12	3.14±0.29	4.03±0.41	2.17±0.22	1.30±0.13	1.49±0.15
			40	65	2.81±0.22	0.30±0.05	3.11±0.31	1.31±0.16	1.55±0.16	2.87±0.28	2.13±0.21	0.19±0.02	1.08±0.12
			60	69	2.72±0.30	0.72±0.08	3.44±0.38	1.90±0.18	2.56±0.30	4.46±0.44	1.43±0.14	0.28±0.03	0.77±0.09
			80	40	2.39±0.26	0.65±0.07	3.05±0.29	1.39±0.16	2.35±0.23	3.74±0.38	1.72±0.17	0.28±0.03	0.82±0.08
R20	82°N	169°W	0	25	1.06±0.10	0.37±0.04	1.43±0.12	1.54±0.15	1.43±0.16	2.97±0.30	0.69±0.07	0.26±0.03	0.48±0.05
			10	18	5.29±0.56	0.38±0.04	5.67±0.62	2.22±0.26	1.30±0.13	3.52±0.35	2.38±0.23	0.29±0.03	1.61±0.16
			25	17	4.05±0.38	0.44±0.04	4.49±0.45	2.93±0.30	1.55±0.16	4.48±0.45	1.38±0.16	0.28±0.02	1.00±0.11
			30	9	2.27±0.29	0.34±0.05	2.61±0.27	1.32±0.14	1.33±0.13	2.65±0.23	1.73±0.16	0.25±0.02	0.99±0.10
			75	14	0.85±0.11	0.37±0.04	1.22±0.12	1.06±0.10	2.00±0.20	3.06±0.29	0.81±0.10	0.19±0.02	0.40±0.04
			90	20	1.39±0.14	0.43±0.04	1.82±0.17	1.62±0.15	2.33±0.23	3.96±0.41	0.86±0.10	0.18±0.02	0.46±0.04

Notes: D_{Po} is the activity of dissolved ^{210}Po, P_{Po} the activity of particulate ^{210}Po, T_{Po} the activity of total ^{210}Po, D_{Pb} the activity of dissolved ^{210}Pb, P_{Pb} the activity of particulate of ^{210}Pb, and T_{Pb} the activity of total ^{210}Pb. $^{210}Po/^{210}Pb_{A.R.}$ is the activity ratio of ^{210}Po to ^{210}Pb.

Table 2 Inventory of particulate and dissolved ^{210}Po and ^{210}Pb in euphotic zone, and residence time and export fluxes of particulate and dissolved ^{210}Po

Station	Euphotic layer (m)	I_{DPo}	I_{PPo}	I_{DPb}	I_{PPb}	J_{Po}	P_{Po}	τ_{DPo}	τ_{PPo}
		(Bq/m^2)				(Bq/(m^2·a))		(a)	
R03	30	53.70	15.15	43.73	47.18	-18.20	40.26	-2.95	0.38
R09	30	71.10	39.08	37.88	104.18	-60.63	58.18	-1.17	0.67
R12	40	78.00	59.40	71.80	86.80	-11.32	38.69	-6.89	1.54
R20	75	202.80	28.50	136.05	114.15	-121.82	34.49	-1.66	0.83

Notes: I_{DPo}, I_{PPo}, I_{DPb} and I_{PPb} are inventories of dissolved ^{210}Po, particulate ^{210}Po, dissolved ^{210}Pb and particulate ^{210}Pb above the euphotic zone, respectively; J_{Po} is the scavenging flux of dissolved ^{210}Po; P_{Po} is export flux of particulate ^{210}Po; τ_{DPo} and τ_{PPo} are residence times of particulate and dissolved ^{210}Po, respectively.

especially advective processes, is important for ^{210}Pb, owing to its half-life of 22.3 years (Friedrich et al., 2002; Kim et al., 2012). The spatially comparable activity of ^{210}Po and ^{210}Pb further constrains the fluxes because of advective processes, which are minor relative to vertical fluxes.

An irreversible, steady state model of ^{210}Po was built without advective and diffusive items and atmospheric deposition. To estimate the rates of ^{210}Po and ^{210}Pb scavenged by suspended particles and their removal via sinking particles, the following equations were used for the disequilibrium between ^{210}Po and ^{210}Pb in seawater (Bacon et al., 1976):

$$J=\lambda_{Po}\ (I_{DPb}-I_{DPo}), \quad (1)$$

$$P=\lambda_{Po}\ (I_{PPb}-I_{PPo})+J, \quad (2)$$

where J is the scavenging flux of dissolved ^{210}Po; λ_{Po} is the decay constant (0.005/d) of ^{210}Po; I_{DPo} and I_{DPb} are the inventory of dissolved ^{210}Po and ^{210}Pb, respectively; P is the export flux of particulate ^{210}Po; I_{PPo} and I_{PPb} are the inventory of particulate ^{210}Po and ^{210}Pb. The residence times of particulate and dissolved ^{210}Po are given by

$$\tau_{DPo}=I_{Dpo}/J, \quad (3)$$

$$\tau_{PPo}=I_{Ppo}/P. \quad (4)$$

Based on Eqs.1–4, J, P, τ_{DPo}, and τ_{PPo} are presented in Table 2. This shows that mean residence times of particulate and dissolved ^{210}Po in the euphotic zone of different stations were almost all negative, which may be caused by regeneration of particles (He et al., 2008). However, the residence time of particulate ^{210}Po was higher than that of dissolved ^{210}Po, indicating rapid biogeochemical cycling in the study area (Rutgers van der Loeff et al., 1995).

3.3 Distribution of particulate organic carbon concentrations

Concentrations of POC in the water column are given in Table 1. POC concentration was 9–601 μg C/L in the study area, with average 106 μg C/L. The highest concentration of 601 μg C/L were found at R03 during the first sampling period, this decreased northwards and offshore during the second sampling period, consistent with the distribution of chlorophyll-*a* (Yu et al., 2012). POC concentrations in surface water were lower than in deeper water, owing to sediment resuspension (Yu et al., 2012).

3.4 POC export fluxes from euphotic zone

The distribution of POC export fluxes in the Arctic Ocean has significant temporal and regional variability (Yu et al., 2012). Export fluxes of particulate ^{210}Po and its residence time in the euphotic zone were calculated in the irreversible scavenging model (Yang, 2005). Furthermore, POC export fluxes were calculated with the ratio of POC content to activity of ^{210}Po, per the equation of Buesseler et al. (1992) and Yang (2005):

$$B_{POC\text{-}flux}=f_{POC}=f_{Po}\times r, \quad (5)$$

where f_{Po} is the export flux of particulate ^{210}Po and r is the ratio of content of POC to activity of ^{210}Po at the bottom of the euphotic zone. With this equation, we hypothesized that the carriers of ^{210}Po and POC were the same particle but not that they have similar geochemical behaviors. Apparently, the former hypothesis was easily satisfied in the study area. The export fluxes and the residence times of ^{210}Po are listed in Table 2, and the POC fluxes (Method B, marked with $B_{POC\text{-}flux}$) are given in Table 3. At station R03, the residence time of ^{210}Po was the shortest, only 0.38 a, and the POC export flux was the highest, at 1 848 mmol C/(m^2·a). The latter may have been caused by the upwelling in the area (Yu, 2010).

Another equation to calculate POC export flux at steady state was developed by Eppley (1979), which assumes the residence time of ^{210}Po and POC as

$$E_{POC\text{-}flux}=f_{POC}=f_{POCinv}/\tau_{PPo}, \quad (6)$$

where the f_{POCinv} is export flux of the POC inventory in the euphotic zone. The results (Method E, marked by $E_{POC\text{-}flux}$) derived from Eq.6 are listed in Table 3. Compared with the export fluxes derived from method B, the results calculated by different methods are almost equal (within 40%; He et al., 2008). Considering errors for the activities of ^{210}Po and content of POC, we assume that the results derived by the above two methods are consistent.

Average POC export fluxes 945 mmol C/(m^2·a) (Method E) and 1 848 mmol C/(m^2·a) (Method B) in the euphotic zone at R03 were much higher than those at R20, 126 mmol C/(m^2·a) (Method E) and 109 mmol C/(m^2·a) (Method B). This shows a decreasing trend northward, comparable to prior work in the same region (Yu et al., 2012). Compared with other reported POC export fluxes (Table 3) in certain areas of the world ocean based on various approaches, the fluxes on the Chukchi Shelf in summer were very high. It is concluded that there is high export production on the Chukchi Shelf in summer. Because available light limits marine primary production at high latitude, this production is increased by sea ice melt during summer. Seawater in the Chukchi Sea is derived from the Bering Sea, with substantial nutrients to support primary production. Consequently, the Chukchi Shelf has a significant role as CO_2 sink during summer.

4 CONCLUSION

In the present study, average dissolved ^{210}Pb at different stations had an increasing trend northward from 1.12 to 1.78 Bq/m^3 during July and August, and average particulate ^{210}Pb 2.22 Bq/m^3 was higher than dissolved ^{210}Pb, at 1.49 Bq/m^3. Residence time of particulate ^{210}Po was greater than that of dissolved ^{210}Po, indicating rapid biogeochemical cycling in the study area. The highest concentration of POC (601 μg C/L) was at station R03 during the first sampling period, which decreased northward during the second sampling period, consistent with the distribution of chlorophyll-*a*. Average POC export fluxes in the euphotic zone were derived by two methods with an irreversible scavenging model. These fluxes had a decreasing trend northward and were comparable to prior work in the study area. This suggests an efficient biological pump in the Arctic Ocean and confirms relatively high new production in that ocean during summer, indicative of a significant role as CO_2 sink. The results may expand knowledge of the carbon cycle in the western Arctic Ocean.

Table 3 Inventory and POC export fluxes in euphotic zone, and summary of POC export fluxes in areas of the world ocean

Station	Time	Euphotic layer (m)	POC inventory (mmol/m^2)	POC/P_{Po} (mmol/Bq)	$E_{POC\text{-}flux}$ (mmol C/(m^2·a))	$B_{POC\text{-}flux}$ (mmol C/(m^2·a))	Reference
R03	July, 2010	0–30	355.70	45.91	945±350	1 848±848	This work
R09	July, 2010	0–30	437.50	17.44	651±514	1 015±015	
R12	Aug, 2010	0–40	129.17	18.06	84±4.	699±990	
R20	Aug, 2010	0–75	103.75	3.15	126±26	109±09	
Prydz Bay (March, 2008)					12 045–108 551		Ma et al., 2014
Prydz Bay (Jan.–Feb., 2006)					19 000–67 525	10 767–95 776	He et al., 2008
Chukchi Shelf (July–Sep., 2008)					3 029–28 908		Yu, 2010
Chukchi Shelf (Aug.–Sep., 1994)					13 870		Moran et al., 1997
Chukchi Continental (Aug.–Sep., 1994)					292–14 235		Moran et al., 2005
Chukchi Continental (July–Sep., 2008)					657–912.5		Yu, 2010
Chukchi Continental (Aug.–Sep., 1994)					1 533–20 878		Trimble and Baskaran, 2005
Canada Basin (July–Sep., 1999)					365		Chen et al., 2003
Canada Basin (Aug., 2000)					511		Trimble and Baskaran, 2005
Western Arctic (1998)					2 701–4 635.5		Baskaran et al., 2003
Subarctic northwest of North Pacific Ocean (May 1996, Feb. 1997, Aug. 1996)					1 022–2 591		Charetee et al., 1999
Weddle Sea (Spring bloom of 1992)					7 300–14 600		Rutgers Van Der Loeff et al., 1997

5 ACKNOWLEDGMENT

We thank the captain and crew members of R/V *Xuelong* and members of the oceanographic group for onboard assistance during CHINARE-4.

References

Anderson L G, Olsson K, Chierica M. 1998. A carbon budget for the Arctic Ocean. *Global Biochemistry*, **12**(3): 455-465.

Bacon M P. 1976. Applications of Pb-210/Ra-226 and Po-210/Pb-210 Disequilibria in the Study of Marine Geochemical Processes. Ph. D. Thesis, MIT-WHOI. 165p.

Balkanski Y J, Jacob D J, Gardner G M, Graustein W C, Turekian K K. 1993. Transport and residence times of troposphere aerosols inferred from a global three-dimensional simulation of ^{210}Pb. *Journal of Geophysical Research*, **98**(D11): 20 573-20 586.

Baskaran M, Naidu A S. 1995. ^{210}Pb-derived chronology and the fluxes of ^{210}Pb and ^{137}Cs isotopes into continental shelf sediments, East Chukchi Sea, Alaskan Arctic. *Geochimica et Cosmochimica Acta*, **59**(21): 4 435-4 448.

Baskaran M, Santschi P H. 2002. Particulate and dissolved ^{210}Pb activities in the shelf and slope regions of the Gulf of Mexico waters. *Continental Shelf Research*, **22**: 1 493-1 510.

Baskaran M, Swarzenski P M, Porcelli D. 2003. Role of colloidal material in the removal of ^{234}Th in the Canada basin of the Arctic Ocean. *Deep Sea Research I*, **50**(10): 1 353-1 373.

Baskaran M. 2011. Po-210 and Pb-210 as atmospheric tracers and global atmospheric Pb-210 fallout: a review. *Journal of Environmental Radioactivity*, **102**: 500-513.

Bates N R. 2006. Air-sea CO_2 fluxes and the continental shelf pump of carbon in the Chukchi Sea adjacent to the Arctic Ocean. *Journal of Geophysical Research*, **111**(C10013), http://dx.doi.org/10.1029/2005JC003083.

Buesseler K O, Bacon M P, Cochran J K, Livingston H D. 1992. Carbon and nitrogen export during the JGOFS North Atlantic Bloom experiment estimated from ^{234}Th:^{238}U disequilibria. *Deep Sea Research Part I*, **39**: 1 115-1 137.

Buesseler K O, Benitez-Nelson C R, Rutgers van der Loeff M M, Andrews J, Ball L, Crossin G, Charette M A. 2001. An intercomparison of small- and large-volume techniques for thorium-234 in seawater. *Marine Chemistry*, **74**: 15-28.

Cai P, Chen W, Dai M, Wan Z, Wang D, Li Q, Tang T, Lv D. 2008. A high-resolution study of particle export in the southern South China Sea based on ^{234}Th:^{238}U disequilibrium. *Journal of Geophysical Research*, **113**: C04019, http://doi:10.1029/2007JC004268.

Cai P, Dai M, Lv D, Chen W. 2006. An improvement in the small-volume technique for determining thorium-234 in seawater. *Marine Chemistry*, **100**: 282-288.

Cai P, Huang Y, Chen M, Guo L, Liu G, Qiu Y. 2002. New production based on ^{228}Ra-derived nutrient budgets and thorium-estimated POC export at the intercalibration station in the South China Sea. *Deep Sea Research I*, **49**: 53-66.

Cai W J, Chen L, Chen B, Gao Z, Lee S H, Chen J, Pierrot D, Sullivan K, Wang Y, Huang W J, Zhang Y, Xu S, Murata A, Grebmeier J M, Jones E P, Zhang H. 2010. Decrease in the CO_2 uptake capacity in an ice-free Arctic Ocean basin. *Science*, **329**(5991): 556-559.

Carvalho F P. 2011. Polonium (^{210}Po) and lead (^{210}Pb) in marine organisms and their transfer in marine food chains. *Journal of Environmental Radioactivity*, **102**(5): 462-472.

Charette M A, Moran S B, Bishop J K. 1999. ^{234}Th as a tracer of particulae organic carbon export in the subarctic northeast Pacific Ocean. *Deep Sea Research II*, **46**(11-12): 2 833-2 861.

Chen M, Huang Y P, Cai P H, Guo L. 2003. Particulate organic carbon export fluxes in the Canada Basin and Bering Sea as derived from $^{234}Th/^{238}U$ disequilibria. *Arctic*, **56**(1): 32-44.

Coale K H, Bruland K W. 1985. $^{234}Th:^{238}U$ disequilibria within the California Current. *Limnology and Oceanography*, **30**(1): 22-33.

Eakins J D, Morrison R T. 1978. A new procedure for the determination of lead-210 in lake and marine sediments. *The International Journal of Applied Radiation and Isotopes*, **29**(9-10): 531-536.

Else B G T, Papakyriakou T N, Granskog M A et al. 2008. Observations of sea surface fCO_2 distributions and estimated air-sea CO_2 fluxes in the Hudson Bay region (Canada) during the open water season. *Journal of Geophysical Research*: *Oceans (1978–2012)*, **113**(C8).

Eppley R W, Peterson B J. 1979. Particulate organic matter flux and planktonic new production in the deep ocean. *Nature*, **282**: 677-680.

Fleer A P, Bacon M P. 1984. Determination of ^{210}Pb and ^{210}Po in seawater and marine particulate matter. *Neclear Instrumentation and Methods of Physical Research*, **223**(2-3): 243-249.

He J, Ma H, Chen L, Xiang B, Zeng X, Yin M, Zeng W. 2008. The investigation on particulate organic carbon fluxes with disequilibria between thorium-234 and uranium-238 in Prydz Bay, the Southern Ocean. *Acta Oceanologica Sinica*, **27**(2): 21-29.

Kim G, Kim T-H, Church T M. 2012. Po-210 in the environment: biogeochemical cycling and bioavailability. *In*: Baskaran M ed. Handbook of Environmental Isotope Geochemistry, Advances in Isotope Geochemistry. p.271-284.

Liu Z L, Chen J F, Zhang T, Chen Z, Zhang H. 2007. The size-fractionated chlorophyll *a* concentration and primary productivity in the Chukchi Sea and its northern Chukchi Plateau. *Acta Ecological Sinica*, **27**(12): 4 953-4 962.

Ma H, Zeng Z, He J, Han Z, Lin W, Chen L, Cheng J, Zeng S. 2014. ^{234}Th-derived particulate organic carbon export in the Prydz Bay, Antarctica. *Journal of Radioanalytical and Nuclear Chemistry*, **299**: 621-630.

Masque P, Cochran J K, Hirschberg D J et al. 2007. Radionuclides in Arctic sea ice: tracers of sources, fates and ice transit time scales. *Deep Sea Research Part I*: *Oceanographic Research Papers*, **54**(8): 1 289-1 310.

Masque P, Sanchez-Cabeza J A, Bruach J M , Palacois E, Canals M. 2002. Balance and residence times of Pb-210 and Po-210 in surface waters of the northwestern Mediterranean Sea. *Continental Shelf Research*, **22**: 2 127-2 146.

Moran S B, Ellis K M, Smith J N. 1997. $^{234}Th/^{238}U$ disequilibrium in the central Arctic Ocean: implications for particulate organic carbon export. *Deep Sea Research II*, **44**(8): 1 593-1 606.

Moran S B, Kelly R P, Hagstrom K, Smith J N, Grebmeier J M, Cooper L W, Cota G F, Walsh J J, Bates N R, Hansell D A, Maslowski W, Nelson R P, Mulsow S. 2005. Seasonal changes in POC export flux in the Chukchi Sea and implications of water column-benthic coupling in Arctic shelves. *Deep Sea Research II*, **52**: 3 427-3 451.

Nozaki Y. 1986. Ra-226–Rn-222–Pb-210 systematics in seawater near the bottom of the ocean. *Earth and Planetary Science Letters*, **80**: 36-40.

Pipko I I, Semiletov I P, Tishchenko P Y et al. 2002. Carbonate chemistry dynamics in Bering Strait and the Chukchi Sea. *Progress in Oceanography*, **55**(1): 77-94.

Rutgers van der Loeff M M, Friedrich J, Bathmann U V. 1997. Carbon export during the spring bloom at southern polar front, determined with the natural tracer ^{234}Th. *Deep Sea Research II*, **44**(1-2): 457-478.

Rutgers van der Loeff M M, Key R M, Scholten J, Bouch D, Michel A. 1995. ^{228}Ra as a tracer for shelf water in the Arctic Ocean. *Deep Sea Research II*, **42**(6): 1 533-1 553.

Rutgers van der Loeff M M, Meyer R, Rudels B, Rachor E. 2002. Resuspension and particle transport in the benthic nepheloid layer in and near Fram Strait in relation to faunal abundances and ^{234}Th depletion. *Deep Sea Research I*, **49**(11): 1 941-1 958.

Shimmield G B, Ritchie G D, Fileman T W. 1995. The impact of marginal ice zoneprocesses on the distribution of ^{210}Po, ^{210}Pb and ^{234}Th and implications for new production in the Bellingshausen Sea, Antarctica. *Deep Sea Research II*, **42** (4-5): 1 313-1 335.

Stewart G, Moran S, Lomas M, Kelly R. 2011. Direct comparison of ^{210}Po, ^{234}Th and POC particle-size distributions and export fluxes at the Bermuda Atlantic Time-series study (BATS) site. *J. Environ. Radioact*., **102**: 479-489.

Trimble S M, Baskaran M. 2005. The role of suspended particulate matter in ^{234}Th scavenging and ^{234}Th-derived export fluxes of POC in the Canada Basin of the Arctic Ocean. *Marine Chemistry*, **96**: 1-19.

Verdeny E, Masque P, Garcia-Orellana J, Hanfland C, Cochran J K, Stewart G M. 2009. POC export from ocean surface waters by means of $^{234}Th/^{238}U$ and $^{210}Po/^{210}Pb$ disequilibria: a review of the use of two radiotracer pairs. *Deep Sea Research II*, **56**: 1 502-1 518.

Woodgate R, Aagaard K, Weingartner T. 2005. A year in the physical oceanography of the Chukchi Sea: Moored measurements from autumn 1990–1991. *Deep Sea Research II*, **52**: 3 116-3 149.

Yang W F. 2005. Marine Biogeochemistry of ^{210}Po and ^{210}Pb and Their Implications Regarding the Cycling and Export of Particles. Ph. D. Thesis, Xiamen University. (in Chinese with English abstract)

Yang Y L, Han X, Kusakabe M. 2004. POC fluxes from euphotic zone estimated from ^{234}Th deficiency in winter in the north-western North Pacific Ocean. *Acta Oceanologica Sinica*, **23**(1): 135-147.

Yu W, He J, Li Y, Lin W, Chen L. 2012. Particlate organic carbon export fluxes and validation of steady state model of ^{234}Th export in the Chukchi Sea. *Deep Sea Research II*, **81-84**: 63-71.

Yu W. 2010. Estimation and Determination of Carbon Fluxes on Three Interfaces of Western Arctic Ocean in Summer Time. Ph. D. Thesis, Tsinhua University. (in Chinese with English abstract)